

Characterization and deflection missions of the fictitious asteroid 2019 PDC

Javier Roa^{a,1,*}, Anastassios E. Petropoulos^{a,2}, Paul W. Chodas^{a,3}

^a*Jet Propulsion Laboratory, California Institute of Technology, 4800 Oak Grove Dr, Pasadena, CA 91109*

Abstract

The fictitious asteroid 2019 PDC could potentially collide with Earth in April 2027, eight years after discovery in 2019. A simulated end-to-end planetary defense campaign is designed to mitigate the risk of impact. The first phase of the campaign consists in characterizing the size and shape of the asteroid via fast reconnaissance flyby missions. Being able to launch a reconnaissance spacecraft in just two years after the impact probability rises enough to trigger the planetary defense protocol becomes a key factor because it allows reaching the asteroid as early as December 2021. If this launch opportunity is missed, reconnaissance data will not be available until late-2023. A flyby mission should ideally be followed by a rendezvous mission that would provide a reliable estimate of the mass of the asteroid. The second phase of the campaign aims at deflecting the asteroid off its collision course. The present paper focuses on the use of one or several kinetic impactors and does not consider deflection with a nuclear device. Accurate estimates of the physical properties of the asteroid are required at this stage for the successful outcome of the deflection phase, minimizing the risk of disrupting the asteroid or failing to divert the impact location away from Earth. Both westward and eastward deflections are considered, although the latter significantly outperforms the former in terms of how much the impact point is displaced. Rendezvous missions can arrive at the asteroid a few months before deflection to monitor the impact and retrieve valuable data about its post-deflection state. The third phase of the campaign assesses the deflection performance and determines whether a final mission carrying a nuclear device needs to be launched to disrupt the asteroid just a few months before impact.

Keywords: kinetic impactor, rendezvous, flyby, reconnaissance, asteroid deflection

*Corresponding author

Email addresses: javier.roa@jpl.nasa.gov (Javier Roa), anastassios.e.petropoulos@jpl.nasa.gov (Anastassios E. Petropoulos), paul.w.chodas@jpl.nasa.gov (Paul W. Chodas)

¹Navigation Engineer, Solar System Dynamics Group

²Mission Design Engineer, Outer Planet Mission Analysis Group

³Manager, Center for Near Earth Object Studies

©2019. California Institute of Technology. Government sponsorship acknowledged.

1. Introduction

The emergency response exercise conducted during the 2019 IAA Planetary Defense Conference is based on the assumption that the fictitious asteroid 2019 PDC could impact the Earth on April 29, 2027.⁴ The asteroid was supposedly discovered on March 26, 2019, and it will reach the Earth with a relative velocity of approximately 20 km/s along an inbound trajectory. The encounter occurs when the asteroid arrives at its descending node, as depicted in Fig. 1. This figure presents a schematic view of the orbit of the asteroid compared to the orbits of the Earth, Mars, and Venus. The dashed line represents the line of nodes. The asteroid completes three revolutions between discovery in 2019 and impact in 2027 given its orbital period of 971 days (2.66 years).

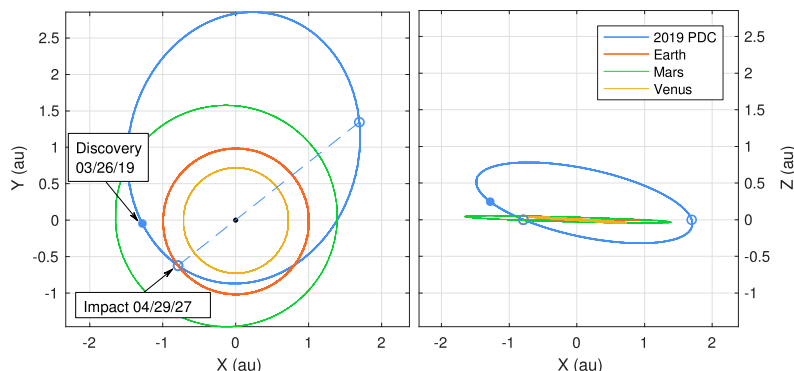


Figure 1: Orbit of asteroid 2019 PDC in the ecliptic ICRF/J2000 frame

With approximately eight years of warning time, different risk mitigation strategies can be implemented in an attempt to divert the collision course of the asteroid away from Earth. Some examples are deflection with pure kinetic energy [1], detonating standoff nuclear devices [2], or transferring momentum to the asteroid with an ion-beam [3]. In particular, kinetic-impactor (KI) missions have been widely studied in the past [4, 5, 6] and constitute a flexible and relatively robust approach. Furthermore, the DART spacecraft plans to validate the concept by impacting the binary asteroid (65803) Didymos as part of the AIDA concept [7, 8]. The present paper focuses on kinetic deflection due to the maturity of this concept. Deflecting the asteroid by detonating a nuclear device is a reasonable alternative although it is not considered in the present paper.

Deflecting the asteroid relying on pure kinetic energy requires high-velocity impacts, large spacecraft masses, or a combination of the two to maximize the momentum exchange. The main limitations of this technique relate to the physical properties of the asteroid. First, the structural properties of the asteroid limit the impact velocity that it can withstand without being disrupted. Uncertainties in the size, density, mass, and composition of the asteroid lead to inaccurate estimates of the limitations of kinetic deflection (see Ref. [9] for a dedicated study). Similarly, it is hard to quantify the effect of material being ejected from the surface or the effect of a partial breakup. Second, the effective deflection attained by a KI mission is proportional to the asteroid's mass. Preliminary estimates of the size of 2019 PDC predict that its diameter can range from 100 up to 300 m, which translates into a difference of almost a factor of 30 between the minimum and maximum possible masses. Such variability complicates the definition of the requirements of the KI mission.

From a mission design perspective, the high orbital inclination of 2019 PDC (18 deg above the ecliptic plane, see Table 1a) makes the asteroid particularly hard to reach due to the high cost of the plane-change maneuvers, especially for rendezvous. Thus, the dates when the asteroid crosses the ecliptic at its ascending or descending nodes become interesting for flyby mission concepts because targeting the nodes minimizes the maneuvers required to tilt the orbital plane. However, the normal component of the velocity of the asteroid at the nodes is significant and, unless the orbital inclination

⁴<https://cneos.jpl.nasa.gov/pd/cs/pdc19/>

of the spacecraft is increased to some extent, it leads to relative velocities at arrival of the order of 20 km/s. Such high relative velocities would make it more difficult to take extensive measurements of the asteroid. Table 1b lists the dates when the asteroid crosses the ecliptic plane, together with the dates of perihelion and aphelion passage since discovery. The Earth crosses the descending node of the orbit of the asteroid at the end of April every year.

Table 1: Definition of the orbit of the fictitious asteroid 2019 PDC

(a) Osculating orbital elements on 2019-Jan-01 (JD 2458484.5)						
a (au)	e	i (deg)	Ω (deg)	ω (deg)	θ (deg)	Period (d)
1.919	0.534	17.997	38.398	226.713	237.350	971

(b) Dates of node crossing and perihelion and aphelion passage			
Descending node	Perihelion	Ascending node	Aphelion
2019-May-07	2019-Jun-11	2019-Dec-28	2020-Oct-09
2022-Jan-02	2022-Feb-06	2022-Aug-25	2023-Jun-07
2024-Aug-30	2024-Oct-04	2025-Apr-22	2026-Feb-02
2027-Apr-29 (Impact)			

Campaign architecture

The simulated impact probability climbs to 10% in mid-2019 and activates the development of a planetary defense campaign. Initially, the uncertainties of the orbit of the asteroid and its physical properties are too large to accurately assess the requirements of a deflection mission. Consequently, the first phase of the campaign consists of reconnaissance missions whose objective is to refine the orbit solution and obtain an estimate of the size, mass, composition, and shape of the asteroid. Two different mission profiles will be considered: flyby and rendezvous. Flyby missions can reach the asteroid quickly and return valuable information including low-altitude images and spectroscopic data to determine its size, shape, and composition. Rendezvousing with the asteroid significantly increases the resolution and volume of the data collected by the spacecraft, resulting in a more accurate characterization including an estimate of the mass. However, longer times of flight are required to rendezvous and deflection missions might have to be launched prior to processing the data. Nevertheless, a spacecraft that co-orbits with the asteroid can monitor the impact of the KI and assess the outcome of the deflection.

Time is critical for early reconnaissance missions. We consider both two- and three-year development times after the impact probability reaches 10%, which allow launching the reconnaissance missions in mid-2021 and 2022, respectively. Quantifying the effects of delaying the launch date by one year from 2021 to 2022 will help to determine how much effort should be directed toward expediting the design, fabrication, testing, and integration phases.

The second phase of the planetary-defense campaign would be the deflection of the asteroid relying on KI missions. Ideally, deflection missions should be launched after processing the data collected by the reconnaissance missions. On the other hand, delaying the launch date potentially reduces the efficiency of the orbit deflection and the optimal trade-off between early and late launch dates should be investigated.

Finally, we outline a contingency plan in case the deflection missions fail to divert the collision course of the asteroid. At that point, all the deflection opportunities would have been missed and the last chance of avoiding an impact would be disrupting the asteroid using a nuclear device. From a mission design perspective, this last-minute mission would be launched after the deflection attempt and it would rendezvous with the asteroid just a few weeks before impact.

2. Reconnaissance mission concepts

The goal of the reconnaissance mission concepts would be to arrive at the asteroid as early as possible to characterize its size, shape, mass, and composition and ultimately determine the requirements of

the deflection missions that would follow. Simplifying the spacecraft design at this stage is crucial to minimize the development time. Reconnaissance missions will most likely rely on a standard, well-tested bus and subsystem architecture. For the design studies conducted in the present section, we assume a spacecraft mass at arrival of 500 kg, which is consistent with the current baseline of the DART mission.⁵ The spacecraft mounts an ion engine that provides continuous low-thrust propulsion. The main advantage of electric propulsion compared to chemical is that it increases the control authority and improves the overall efficiency of the transfers, especially of those involving large plane changes. Hereafter, we adopt the Falcon Heavy launch vehicle (in its expendable configuration) as baseline and limit the departure C_3 to $100 \text{ km}^2/\text{s}^2$ and the declination of the launch asymptote (DLA) to $\pm 28.5 \text{ deg}$, compatible with launches from Cape Canaveral.

2.1. Flyby

Terminal guidance and navigation typically require hyperbolic excess velocities below 20 or 25 km/s [6, 10]. However, for reconnaissance flyby missions we impose a more conservative constraint and limit the arrival velocity to 14 km/s to ensure that the scientific instruments dedicated to characterizing the asteroid operate within usual data acquisition and slew rates. Similarly, the Sun phase angle ϕ at arrival (formed by the v_∞ vector of the spacecraft relative to the asteroid and the heliocentric position vector of the asteroid) shall be less than 90 degrees to ensure that the asteroid is illuminated from the spacecraft point of view. The perihelion distance is constrained to 0.35 au to ensure that the spacecraft orbit does not cross Mercury's orbit, thus limiting the thermal exposure of the spacecraft. The thermal design of the spacecraft will require special attention when considering orbits interior to Earth's.

2.1.1. Flyby missions launched in 2021

First, we consider a two-year development time that allows launching the spacecraft in June 2021. To determine the thrust levels required to fly by the asteroid, we conduct parametric analyses assuming that the thrust is limited to T_{max} for $r < 1.5 \text{ au}$ and that it decreases like $1/r^2$ beyond 1.5 au. The specific impulse is assumed constant, with $I_{\text{sp}} = 3000 \text{ s}$. The thrust is cut off when $r > 3.2 \text{ au}$ to model the minimum-power limit of representative engines.

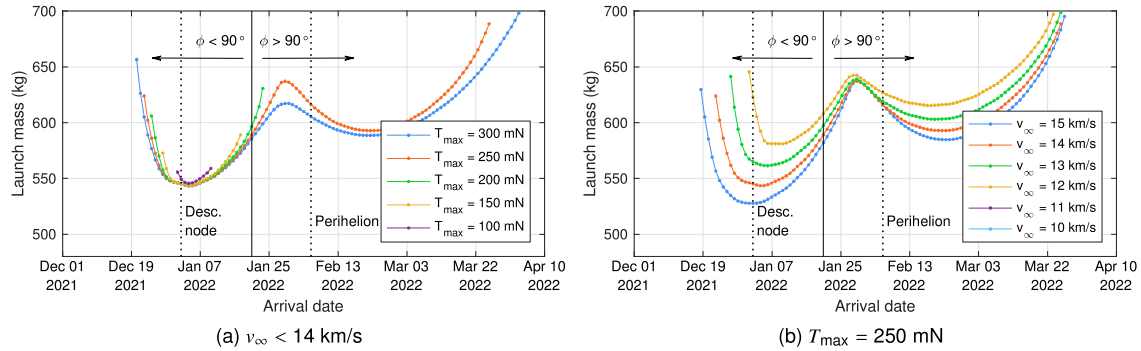


Figure 2: Reconnaissance flyby missions launched in June 2021

Figure 2a shows how early the asteroid can be flown by and the corresponding propellant mass for different values of T_{max} ranging from 100 to 300 mN (Fig. 2a). Each trajectory has been optimized to minimize the launch mass given a fixed arrival date and limiting the launch date to June 1, 2021. Early flyby missions that reach the asteroid close to its 2022 descending node (between December 2021 and January 2022) are feasible even with $T_{\text{max}} = 100 \text{ mN}$. Targeting the descending node minimizes the propellant mass, although some Δv is still required to meet the $v_\infty < 14 \text{ km/s}$ terminal constraint. Increasing the available thrust from 100 mN (earliest arrival on January 1, 2022) up to 300 mN (earliest arrival December 21, 2021) advances the earliest arrival date by approximately 10 days. Missions

⁵<http://dart.jhuapl.edu/The-Spacecraft/index.php>

arriving later than January 21, 2021 no longer satisfy the Sun phase angle constraint ($\phi \leq 90^\circ$). Right before the 2022 perihelion, the launch mass reaches a local maximum that corresponds to the zero-to one-revolution transition. Note that $T_{\max} = 150$ mN and $T_{\max} = 250$ mN are comparable to the performance of the XIPS25 and the NEXT (HiThrust) engines, respectively, with maximum power inputs of 5.1 kW and 7.2 kW. Their specific impulses are approximately 3500 and 4000 s.

Figure 2b is obtained by fixing T_{\max} to 250 mN and changing the constraint on the arrival velocity from 10 to 15 km/s. The results in the figure prove that the constraint on the terminal velocity can become as important as the maximum available thrust; reducing the arrival v_∞ requires accelerating the spacecraft to match the velocity of the asteroid, at the cost of increasing the total Δv imparted to the spacecraft. Faster flybys ($v_\infty = 15$ km/s) in early December 2021 are feasible, while the arrival date shifts to January 2022 for slower flybys ($v_\infty = 10$ km/s).

Figure 3 presents two examples of flyby missions for early reconnaissance with $v_\infty = 13$ km/s using the NEXT engine (Fig. 3a) and the XIPS25 engine (Fig. 3b). In both cases, the duty cycle is 90% and the spacecraft incorporates triple junction gallium-arsenide solar panels providing 6 kW of power at 1 au. The departure date in these examples is fixed to June 1, 2021, and the objective is to minimize the trip time. The thrust delivered by the NEXT engine is higher and results in earlier arrival dates at the cost of increasing the propellant consumption, although the difference between the two arrival dates is just three days. The minimum distance to the Sun is 0.5 au and the arrival Sun phase angle is 53 degrees, a favorable value for terminal guidance.

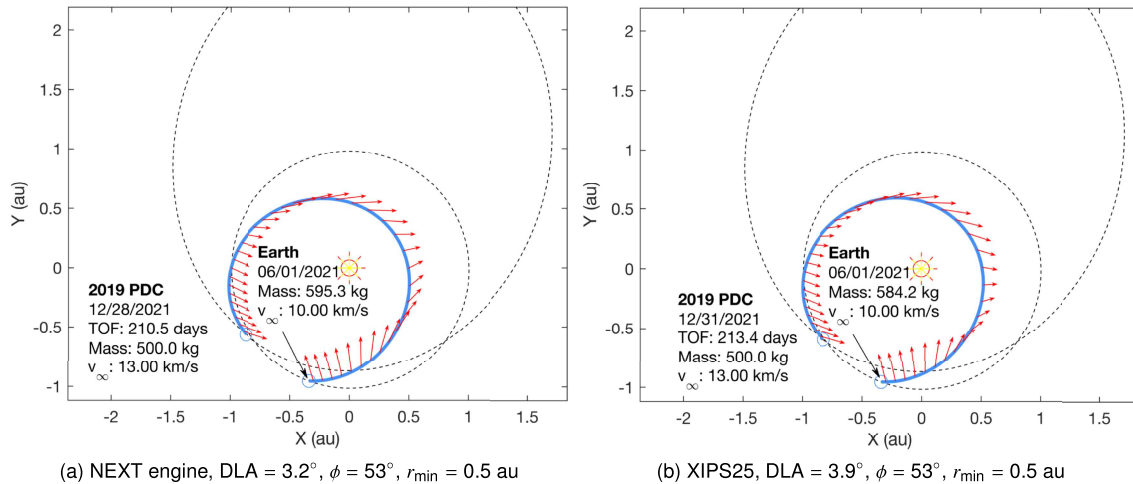


Figure 3: Examples of early reconnaissance flyby missions launched in 2021 (duty cycle 90%, 6 kW at 1 au)

The fastest flyby missions like the ones shown in Fig. 3 are interior transfers that take advantage of the maximum excess velocity that the launch vehicle can provide, $v_\infty = 10$ km/s. Continuous thrust is mostly used to satisfy the terminal velocity constraint. Delaying the launch window while targeting the descending node reduces the time of flight and the minimum distance to the Sun, soon resulting in unfeasible transfers. This is the reason why it is important to keep the development time as short as possible and benefit from this flyby opportunity.

2.1.2. Flyby missions launched in 2022

Allocating three years for developing the spacecraft is a more conservative approach, although it delays the launch window to June 2022. In June 2022, the asteroid will have already passed its perihelion and it will have embarked on an outbound trajectory. As the arrival date moves forward in time, the propellant required to intercept the asteroid decreases because less thrust needs to be invested into reducing the arrival velocity. The velocity of the asteroid at aphelion is low and the relative velocity of the spacecraft at arrival is low too. Figure 4a suggests that, if enough thrust is available, it is possible to fly by the asteroid

before it reaches its aphelion in June 2023. Figure 4b indicates that the terminal velocity is significantly lower than the one observed in the reconnaissance missions arriving in December 2021 (compare to Fig. 2). As a result, the arrival conditions are more favorable for terminal guidance and navigation, with Sun phase angles between 10 and 45 degrees. The minimum time of flight is about one year depending on the thrust level, which is approximately twice than reconnaissance missions launched in 2021.

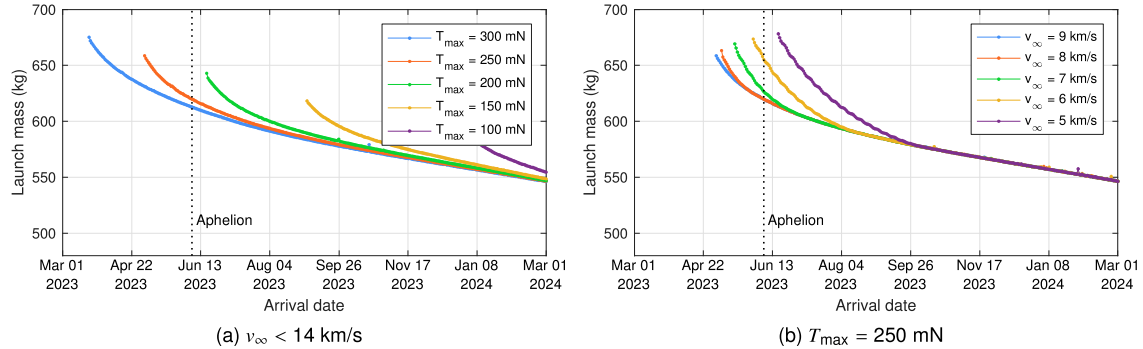


Figure 4: Reconnaissance flyby missions launched in June 2022

Two sample trajectories are depicted in Fig. 5, using the NEXT (Fig. 5a) and XIPS25 engines (Fig. 5b) with 90% duty cycles and 6 kW at 1 au. The missions are launched on June 1, 2022, and the objective is to minimize the transfer time. Both trajectories arrive at the asteroid in December 2023, six months after aphelion. The NEXT engine delivers up to 200 mN whereas the maximum thrust from the XIPS25 engine in this case is 160 mN. The result is a 20-day increase in the time of flight of the latter while reducing the propellant mass by 20% compared to the former. The DLA is -28.5 degrees and the Sun phase angles at arrival are 35 (NEXT engine) and 32 degrees (XIPS25 engine).

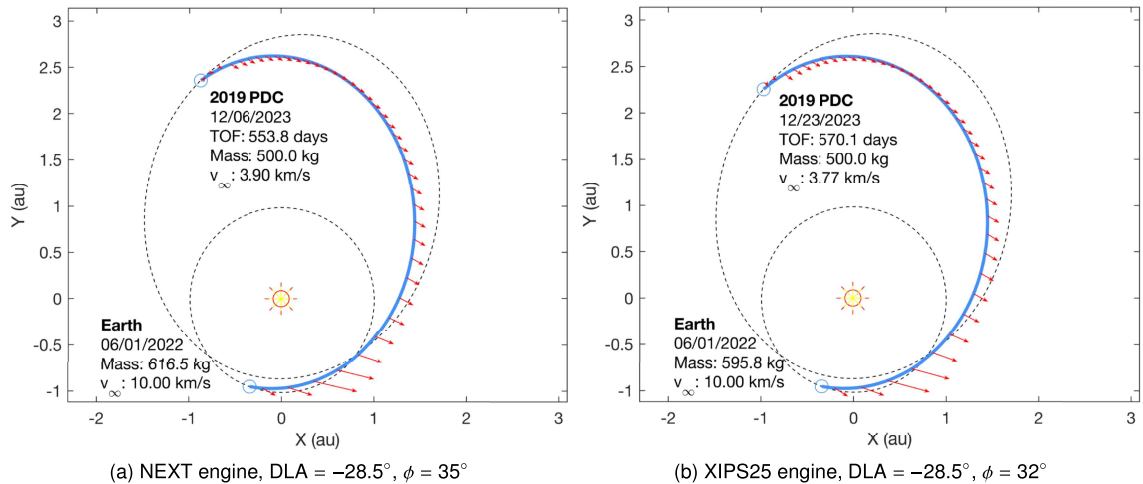


Figure 5: Examples of early reconnaissance flyby missions launched in 2022 (duty cycle 90%, 6 kW at 1 au)

From the moment the asteroid crosses its perihelion in February 2022 up until it approaches aphelion in June 2023, the relative geometry results in arrival conditions that no longer satisfy the terminal constraints (particularly $\phi < 90^\circ$) unless the spacecraft is provided with relatively high thrust levels. The constraints on the time of flight rule out multi-revolution transfers that could alleviate these geometric

challenges. As a result, flyby missions launched in 2022 will typically arrive close to or after aphelion in June 2023.

2.2. Rendezvous

The physical data retrieved during the reconnaissance flybys is limited. For example, a single flyby at roughly 10 km/s will not be sufficient to estimate the gravitational parameter of the asteroid, and therefore its mass. A rendezvous mission provides significantly more scientific data useful for characterizing the asteroid, at the cost of increasing the time of flight in order to match the velocity of the asteroid. More importantly, if the spacecraft stays in the vicinity of the asteroid during the impact of the KI spacecraft, it can assess whether the deflection succeeds or fails.

2.2.1. Rendezvous missions launched in 2021

Under the assumption that reconnaissance missions can be launched as early as June 2021, Fig. 6 indicates that the spacecraft can rendezvous with the asteroid from late-2023 to mid-2024. That is, the time of flight ranges from two and a half to three years, depending on the thrust levels. The propellant mass required for rendezvous decreases as the asteroid moves further away from aphelion and approaches perihelion. Ideally, the launch vehicle will take care of most of the plane change and inject the spacecraft into an elliptical orbit whose energy is as close to the asteroid orbital energy as possible to minimize the relative velocity at arrival. However, the constraints on the DLA and the launch C_3 limit how much the launch vehicle can increase the inclination and the energy, thus requiring continuous thrust to rendezvous with the asteroid.

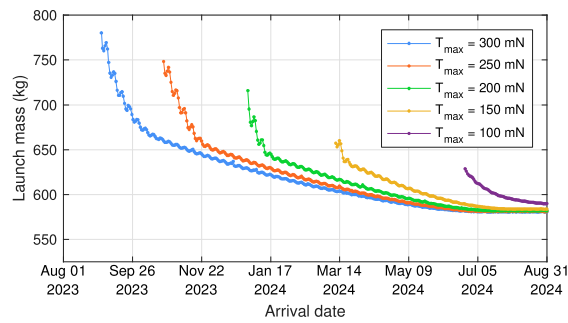


Figure 6: Rendezvous missions launched in June 2021

Imposing a minimum-power constraint causes the thruster to turn off when the power falls below a given threshold. The minimum-power cutoff for the NEXT engine is 0.6 kW and 0.4 kW for the XIPS25 engine. Even though the NEXT engine can deliver a higher thrust, the XIPS25 engine can operate farther away from the Sun where the available power decreases. As a result, using the XIPS25 engine can reduce the time of flight by more than a month compared to using the NEXT engine (see Fig. 7). The aphelion of the trajectories shown in the figure is 3.5 au.

2.2.2. Rendezvous missions launched in 2022

When designing rendezvous missions, the effect of delaying the launch date to June 2022 is significantly smaller than in the case of flyby missions. Comparing Figs. 8 and 6 demonstrates that launching one year later moves the earliest arrival date by a few months but it does not change the overall distribution of solutions. Although the departure date is delayed by one year the arrival date remains effectively the same, therefore reducing the flight time by one year.

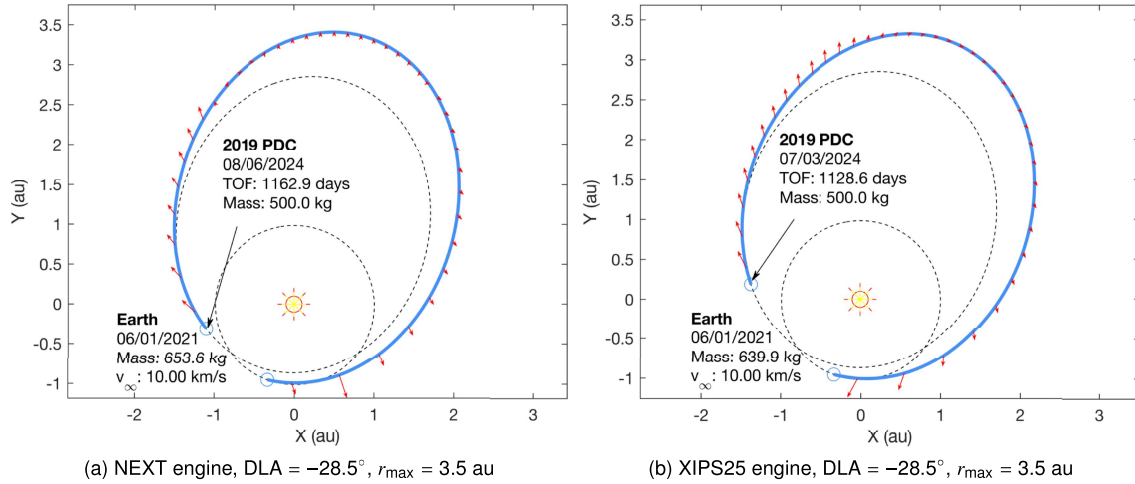


Figure 7: Examples of reconnaissance rendezvous missions launched in 2021 (duty cycle 90%, 6 kW at 1 au)

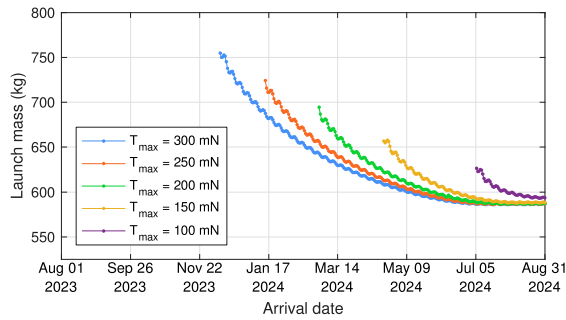


Figure 8: Rendezvous missions launched in June 2022

Moreover, when considering specific engines to design trajectories like those in Fig. 9, reducing the time of flight results in lower aphelia, meaning that the engine can deliver more thrust throughout the mission. As a result, it is possible that missions launched in 2022 will arrive at the asteroid earlier than those launched in 2021 because the spacecraft stays closer to the Sun, where more thrust is available.

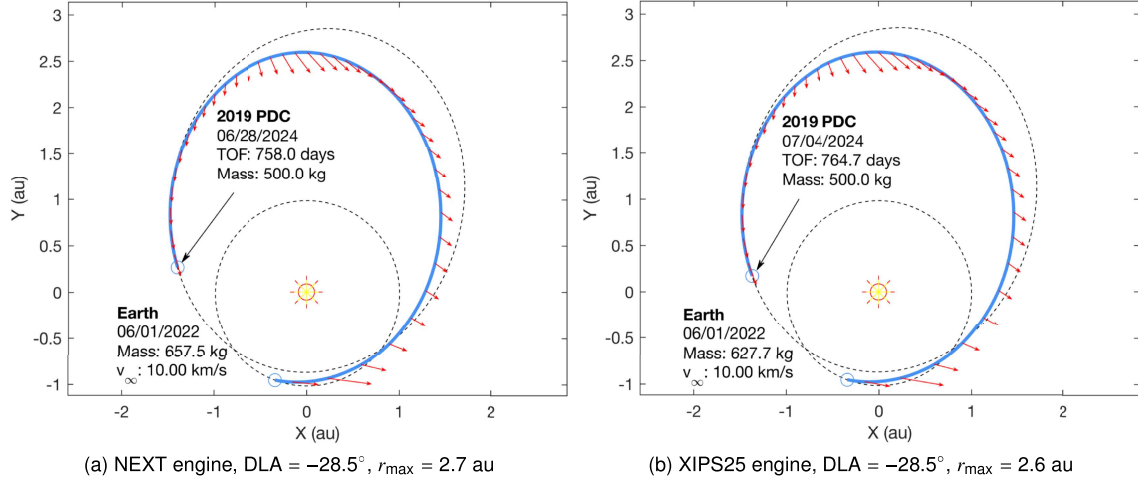


Figure 9: Examples of reconnaissance rendezvous missions launched in 2022 (duty cycle 90%, 6 kW at 1 au)

3. Deflection missions

The exchange of momentum during the impact of a KI with the asteroid at time t^* can be estimated from the conservation of linear momentum in the ideal case:

$$m_{\text{ast}}\mathbf{v}_{\text{ast}} + m_{\text{sc}}\mathbf{v}_{\text{sc}} = (m_{\text{ast}} + m_{\text{sc}})(\mathbf{v}_{\text{ast}} + \Delta\mathbf{v}). \quad (1)$$

Writing the velocity of the spacecraft like $\mathbf{v}_{\text{sc}} = \mathbf{v}_{\text{ast}} + \mathbf{v}_{\infty}$ leads to

$$(m_{\text{ast}} + m_{\text{sc}})\mathbf{v}_{\text{ast}} + m_{\text{sc}}\mathbf{v}_{\infty} = (m_{\text{ast}} + m_{\text{sc}})(\mathbf{v}_{\text{ast}} + \Delta\mathbf{v}) \implies m_{\text{sc}}\mathbf{v}_{\infty} = (m_{\text{ast}} + m_{\text{sc}})\Delta\mathbf{v} \simeq m_{\text{ast}}\Delta\mathbf{v} \quad (2)$$

because, in general, $m_{\text{ast}} \gg m_{\text{sc}}$. Thus, the net impulse imparted to the asteroid is well approximated by:

$$\Delta\mathbf{v} \simeq \beta \frac{m_{\text{sc}}}{m_{\text{ast}}} \mathbf{v}_{\infty}, \quad (3)$$

where the constant factor β accounts for the momentum transfer efficiency. It depends on the physical properties of the asteroid, the dynamics of ejected material, etc. To compute the effective $\Delta\mathbf{v}$ applied to the asteroid, we take $\beta = 1$, which corresponds to a perfectly plastic collision. The mass of the asteroid is estimated assuming a spherical shape with diameter $d_{\text{ast}} = 200$ m and density $\rho_{\text{ast}} = 1500$ kg/m³.

Let $\mathbf{b} = [\xi, \zeta]^T$ denote the coordinates of the impact point on the B-plane (see the Appendix for a detailed definition). The ζ -direction opposes the projection of Earth's velocity on the B-plane. How much the location of the impact point moves on the B-plane due to a $\Delta\mathbf{v}$ applied at $t = t^*$ can be estimated via the linear mapping

$$\Delta\mathbf{b} = \left. \frac{\partial \mathbf{b}}{\partial \mathbf{v}} \right|_{t^*} \Delta\mathbf{v}. \quad (4)$$

The linear approximation holds because the asteroid does not experience any close encounter (or any other comparable nonlinear phenomenon) in the time frame of the campaign. The partial derivatives $\partial \mathbf{b} / \partial \mathbf{v}$ measure the sensitivity of the coordinates of the impact point with respect to changes in the velocity. The sensitivity evolves over time.

Projecting the $\Delta\mathbf{v}$ onto the alongtrack (A), crosstrack (C), and normal (N) directions provides useful insights. In particular, Fig. 10 represents each of the partial derivatives in Eq. (4), which define the sensitivity of the B-plane coordinates to changes on each of the components of the velocity. The partial derivatives of the ξ -coordinate are represented in blue, whereas the derivatives of ζ are plotted in orange. The partial derivative $\partial \xi / \partial v_A$ dominates over the rest. This means that, in order to maximize

the deflection for a given velocity impulse, the impulse should be aligned with the alongtrack direction, i.e. parallel to the velocity of the asteroid. In addition, most of the deflection occurs along ζ , which is associated with the change in the orbital period of the asteroid, in particular with the delay or advance caused by such changes [11]. This corroborates the well-known result that deflections in the alongtrack direction maximize the asteroid miss distance [5, 12]. Reference [13] presents a comprehensive analysis of the long-term effect that changing the orbital period has on the relative dynamics. In addition, the sensitivity is maximum at perihelion, where impulses maximize the change in orbital energy.

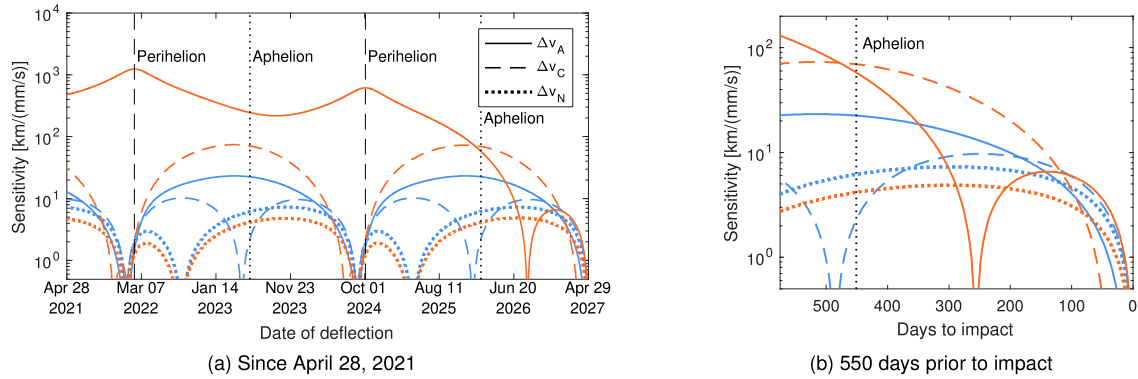


Figure 10: Sensitivity of the B-plane coordinates of the impact point (ξ in blue, ζ in orange) to impulses applied in the alongtrack (A), crosstrack (C), and normal directions (N)

The optimal dates to deflect the asteroid coincide with the dates of perihelion passage, February 2022 and October 2024. An alongtrack impulse applied at perihelion maximizes the change in the orbital period and, with enough time, the phasing difference causes the asteroid to miss the Earth. Targeting the first perihelion passage requires launching the KI mission in 2021 before having processed the characterization data obtained by the reconnaissance missions. Nonetheless, it is worth considering this 2022 deflection opportunity because the expected deflection is two times larger than the 2024 opportunity given the higher sensitivity of the ζ -coordinate.

In addition to deflecting the asteroid by changing its orbital period, it is possible to deflect the asteroid by rotating the orbital plane. Since the impact with Earth occurs at the node, changing the longitude of the node effectively moves the impact point on the B-plane. For a given Δv , the maximum plane change is obtained if the impulse is applied at aphelion and in the crosstrack direction. This phenomenon explains the oscillating behavior of $\partial\zeta/\partial v_C$ and $\partial\xi/\partial v_C$ in Fig. 10, with maximum sensitivity at aphelion and minimum at perihelion. Interestingly, as the date of deflection gets closer to the impact date, the sensitivity to impulses in the alongtrack direction decreases because it relies on how much time delay is accumulated from the time the orbital period changes. Conversely, the crosstrack deflection is not too sensitive to the date of deflection, and dominates over the alongtrack deflection between 450 and 100 days before impact (see the zoomed-in view of the partial derivatives in Fig. 10b). In the last three months prior to impact, the sensitivity to alongtrack and crosstrack impulses becomes comparable again.

KIs arriving at the asteroid with a given alongtrack v_∞ can either increase the asteroid's orbital energy (producing a displacement in the positive ζ -direction) or decrease the energy (displacement in the negative ζ -direction). The former approach is harder to implement as it requires impacting the asteroid from behind with a higher velocity. Conversely, for the latter it suffices to place the spacecraft in front of the asteroid and let the asteroid impact the spacecraft with high relative velocity. Increasing the orbital energy of the asteroid moves the impact location westward, whereas decreasing the orbital energy moves the impact point eastward.

Given the uncertainty in the physical properties of the asteroid, it is unclear how high the impact velocity that the asteroid can sustain is. The Δv impulse is typically limited by the escape velocity of the asteroid [9], although more conservative approaches suggest using 10% of that value as the upper limit. In this section, we do not limit the arrival velocity but rather explore how reducing the v_∞ affects

the performance of the deflection. In case the Δv provided by the KI is too high, a comparable deflection can be achieved by delivering the same total Δv but distributed among several spacecraft arriving close to each other in time. In the linear regime, the total deflection resulting from N KIs reads:

$$\Delta \mathbf{b} = \sum_{i=1}^N \left. \frac{\partial \mathbf{b}}{\partial \mathbf{v}} \right|_{\mathbf{r}_i} \Delta \mathbf{v}_i = \frac{\beta}{m_{\text{ast}}} \sum_{i=1}^N \left. \frac{\partial \mathbf{b}}{\partial \mathbf{v}} \right|_{\mathbf{r}_i} m_{\text{sc},i} \mathbf{v}_{\infty,i}. \quad (5)$$

3.1. Eastward deflection

The orbital energy of the asteroid is greater than Earth's orbital energy. As a result, it is easier for KI missions to impact the asteroid with negative alongtrack v_{∞} . This means that the asteroid is moving faster than the KI and the collision occurs when the asteroid encounters the spacecraft along its path. This strategy simply requires that the orbit of the KI intersects the orbit of the asteroid with adequate phasing and allows for short-duration KI missions.

3.1.1. KI targeting the 2022 descending node

In order to deflect the asteroid at its 2022 descending node, KI missions must be launched in 2021. Limiting the launch date to June 2021 results in maximum transfer times of seven months. The spacecraft will be injected into an interior orbit that lies on the ecliptic plane and will intercept the asteroid in January 2022. Thanks to the transfer being coplanar, no Δv needs to be allocated to change the orbital plane of the KI. Thrusting is only required to reduce the relative velocity at arrival in case it is too high for terminal guidance or to guarantee that the asteroid is not disrupted.

Figure 11 indicates how much the asteroid can be deflected given different T_{max} levels and different constraints on the arrival v_{∞} . The deflection is expressed as the displacement in ζ (note that $|\Delta \xi| \ll |\Delta \zeta| \sim \|\Delta \mathbf{b}\|$), retaining the sign. Increasing the available thrust increases the mass that can be delivered to the asteroid, thus increasing the imparted Δv for the same v_{∞} . The numbers in the figure show the effective Δv attained at the $T_{\text{max}} = 200$ mN level. As long as the asteroid can withstand impacts of such energies without being disrupted, it is possible to deflect the asteroid by more than three Earth radii with a single spacecraft.

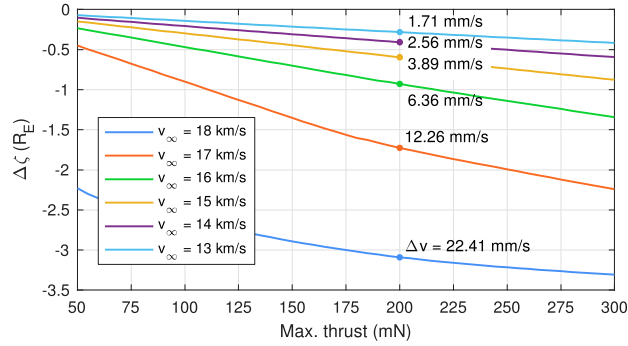


Figure 11: Eastward deflection achieved by KI missions targeting the 2022 descending node

The main driver for KIs targeting the 2022 descending node is the reduced time of flight. If launch dates earlier than June 2021 were feasible, the arrival mass for a given arrival v_{∞} would increase and therefore the deflection would be greater. The deflection modeled according to Eq. (3) is proportional to β , to $1/\rho_{\text{ast}}$ and to $1/d_{\text{ast}}^3$. Thus, deflection maps like Fig. 11 could be easily re-scaled if more accurate estimates of the asteroid's properties were available. For example, using $d_{\text{ast}} = 100$ m instead of $d_{\text{ast}} = 200$ m increases the deflection values in Fig. 11 by a factor of 8.

Two example trajectories are presented in Fig. 12, comparing the performance of the NEXT and XIPS25 engines. The arrival velocity is limited to 17 km/s in this case. The higher thrust of the NEXT engine (Fig. 12a) results in a higher arrival mass when compared to the XIPS25 engine (Fig. 12b). The heavier spacecraft deflects the asteroid by $\Delta \zeta = -1.79 R_E$ on the B-plane, whereas the lighter

spacecraft yields $\Delta\zeta = -1.42 R_E$. The perihelion distance is 0.54 au. The velocity change experienced by the asteroid is approximately 1 cm/s.

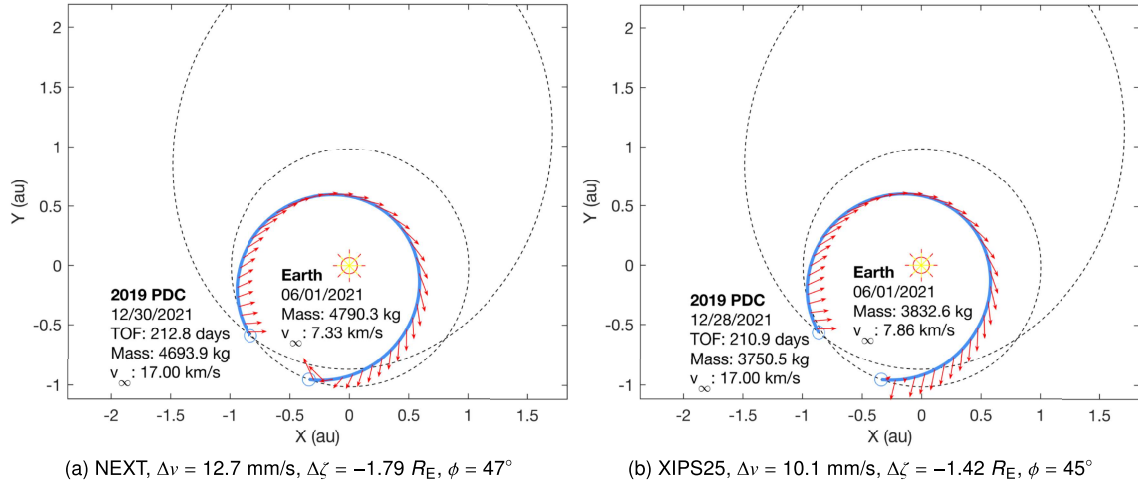


Figure 12: Examples of deflection missions targeting the 2022 descending node (duty cycle 90%, 6 kW at 1 au)

3.1.2. KI targeting the 2024 descending node

The second optimal opportunity to deflect the asteroid is the 2024 descending node (in August). The relative configuration of the problem is similar to that of the 2022 opportunity described in Section 3.1.1. In this case, the launch date is constrained to May 2023, which provides enough time for processing the data retrieved by the 2021 reconnaissance mission.

The longer times of flight (over one year) compared to the KIs targeting the 2022 node results in heavier spacecraft being delivered to the asteroid. For the same v_∞ , the imparted Δv is higher. However, the sensitivity of the ζ -coordinate to changes in the velocity is divided by two (see Fig. 10a). Consequently, the deflection is approximately half of the deflection obtained at the 2022 node. In addition, the orbital energy of the transfer orbit is greater than Earth's, resulting in lower arrival velocities compared to the results in Fig. 11. Although deflecting the asteroid by one Earth radius with a single spacecraft is still possible, the Δv required is higher and might result in the disruption of the asteroid.

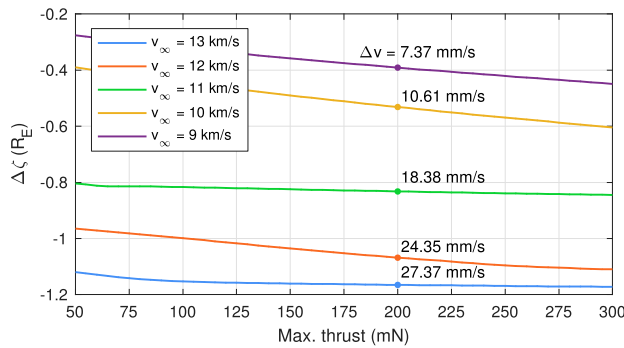


Figure 13: Eastward deflection achieved by KI missions targeting the 2024 descending node

Figure 14 shows two sample missions that deflect the asteroid by a similar amount, using two different engines. The deflection along the ζ -direction is $\Delta\zeta = -1.16 R_E$. The arrival velocity is limited to 13 km/s in these examples, and the Sun phase angle at arrival is 53 deg. The time of flight is longer

than one year and permits transfer orbits with orbital energies greater than Earth's, which are launched with relatively low C_3 .

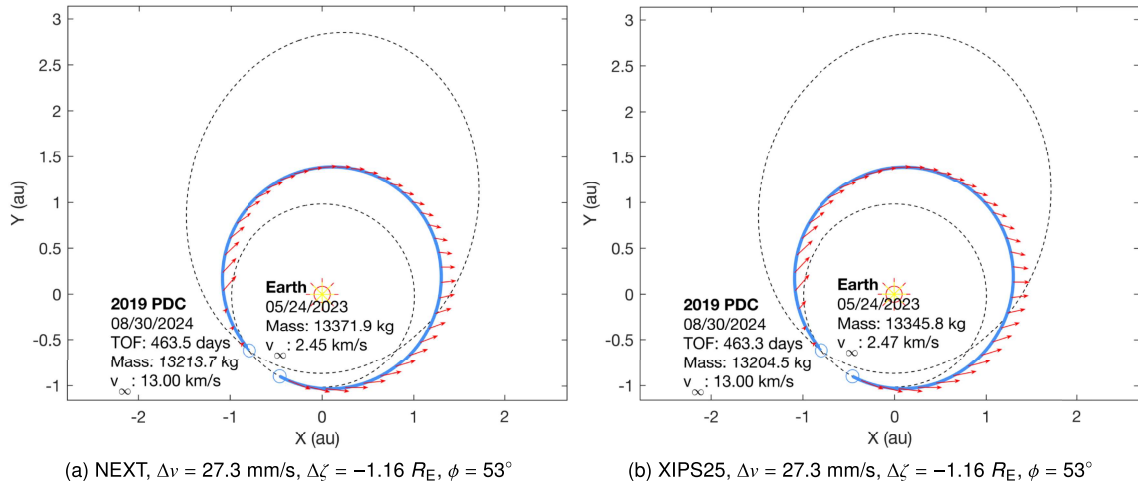


Figure 14: Examples of deflection missions targeting the 2024 descending node (duty cycle 90%, 6 kW at 1 au)

3.2. Westward deflection

To increase the orbital energy of the asteroid and move the impact location westward, the KI must reach the asteroid with a higher orbital speed. Such missions present the same challenges than the rendezvous missions studied in Section 2.2, plus the extra Δv and time of flight required to accelerate the spacecraft beyond what is needed for rendezvous. We force the v_∞ vector at arrival to be parallel to the velocity vector of the asteroid.

The deflection in the positive ζ -direction attainable by missions launched in June 2021 is presented in Fig. 15. Increasing the arrival v_∞ requires accelerating the spacecraft at the cost of reducing the arrival mass. The increasing v_∞ and decreasing arrival mass compensate each other; increasing the arrival v_∞ beyond a certain value no longer increases the momentum transferred to the spacecraft because too much propellant is required to achieve it. This phenomenon suggests that there is an optimal value of the arrival v_∞ that maximizes the deflection, $v_\infty = 3$ km/s in this case. The total Δv imparted to the asteroid is less than 1 mm/s, which leads to maximum deflections of approximately 0.1 Earth radii. To achieve meaningful deflections, significantly more capable launch vehicles will be required to deliver heavier spacecraft with greater relative velocities, like for example SLS Block-IIB. Like in the case of the rendezvous missions, it is possible to launch later than June 2021. However, delaying the launch date reduces the arrival mass and consequently the deflection.

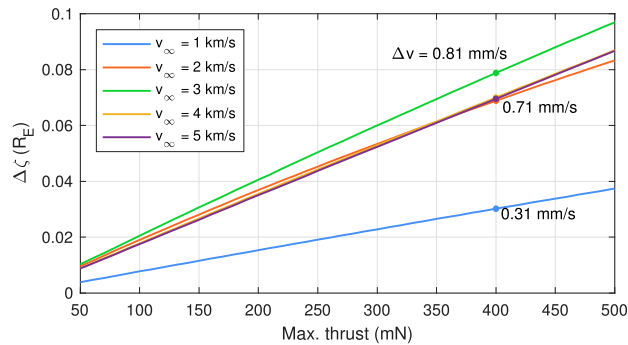


Figure 15: Westward deflection achieved by KI missions targeting the 2024 perihelion

Westward deflections require more thrust than eastward deflections. The two examples in Fig. 16 correspond to spacecraft provided with two engines and producing 10 kW of power at 1 au. Even after increasing the available thrust, the deflection is only 0.04 Earth radii. Although it might not be possible to completely deflect the asteroid westward, this type of deflection missions can move the impact location from the continental United States into the Atlantic Ocean.

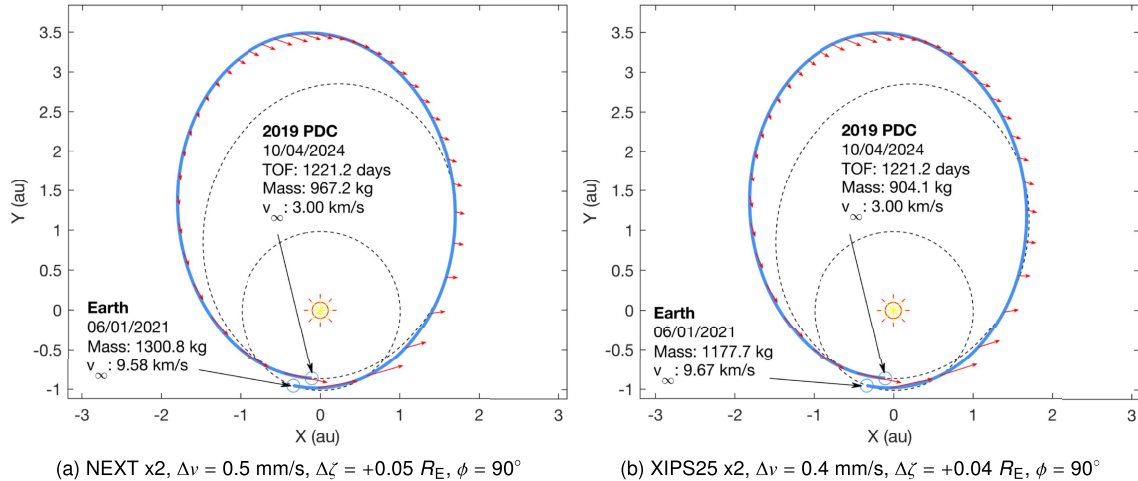


Figure 16: Examples of deflection missions targeting the 2024 perihelion (duty cycle 90%, 10 kW at 1 au)

4. Contingency plan: asteroid disruption with a nuclear device

The nominal KI missions impact the asteroid between August and October 2024. In case they fail to deflect the asteroid, there would not be enough time to send a second campaign of KIs because the asteroid would already be describing its last orbit prior to impact. In addition, the sensitivity of the impact location to velocity impulses drops rapidly and increasingly high impulses would be required for deflection.

Given the time limitations, a reasonable contingency plan is to launch one final mission equipped with a nuclear device to disrupt the asteroid, rather than to deflect it. Enough time should be allocated after the nominal deflection attempts to assess the outcome of the KI missions. The optimal launch window to rendezvous with the asteroid after mid-2024 would be April 2025, which provides between six to eight months after deflection to decide if disrupting the asteroid is advisable and, in that case, finalize the spacecraft configuration.

The spacecraft mass at arrival accounts for the mass of the notional nuclear device. Figure 17 shows how increasing the power throughput can increase the arrival mass, and how the arrival mass decreases the earlier the spacecraft arrives at the asteroid. The missions represented in the figure would be launched in mid-April 2025, and utilize a single NEXT engine with 90% duty cycle. As a reference, a 1000 kg-spacecraft requires 15 kW of power at 1 au to reach the asteroid one month before impact, on March 27, 2029.

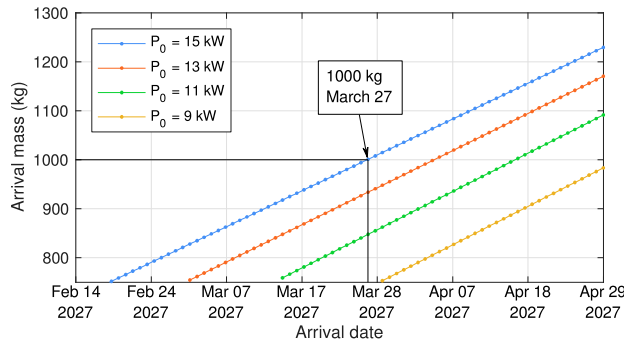


Figure 17: Rendezvous mass delivered prior to impact as a function of the power level at 1 au using one NEXT thruster

5. Nominal campaign architecture

Figure 18 summarizes the architecture of the campaign, which starts when the asteroid impact probability rises to 10%. If the development time of the reconnaissance missions can be reduced down to two years, reconnaissance flyby missions launched in June 2021 can reach the asteroid in December 2021. However, if the spacecraft is not ready to launch until three years after activating the planetary defense protocol, the flyby dates will range from July to December 2023.

Rendezvous missions are less sensitive to the development time. Depending on the thrust the spacecraft is provided with, rendezvous missions can reach the asteroid between late-2023 and mid-2024, typically before the 2024 descending node. The arrival date does not change significantly if the launch date is delayed from 2021 to 2022. The data retrieved by rendezvous missions will not be available before the KI missions are launched, but the spacecraft can monitor the deflection while co-orbiting the asteroid.

There are two opportunities to deflect the asteroid in the eastward direction (negative $\Delta\zeta$). First, KIs launched in June 2021 can deflect the asteroid at its January-2022 descending node. Figure 11 shows that the asteroid can potentially be deflected with a single spacecraft. Second, KIs can target the descending node in August 2024 and the deflection is approximately half of the deflection achieved by the previous set of KIs (see Fig. 13). These missions will be launched in May 2023. Ideally, the data from the reconnaissance flybys would have been available for more than a year. Nonetheless, if the reconnaissance flyby mission misses the 2021 flyby opportunity and its data is not available until September 2023 or later, the launch date of the KI could be delayed at the cost of reducing the deflection. An alternative solution in such case would be to launch the KI as soon as possible before processing the data, and use the data only to optimize the arrival conditions at the asteroid. Given the long time of flight required by rendezvous missions, they will most likely be used to monitor the impact of the KIs rather than to characterize the asteroid prior to launch. The rendezvous spacecraft arrives at the asteroid just a few months before deflection. Finally, to deflect the asteroid westward the KI must be launched in 2021. This strategy results in minimal deflection on the B-plane and its practical interest may reduce to adjusting the impact location on the surface of the Earth.

6. Conclusions

Actions should be taken toward minimizing the mission development time. Being able to launch a reconnaissance flyby mission in two years after activating the planetary defense protocol (in 2021) allows the spacecraft to leverage the favorable orbital geometry and reach the asteroid in just six months (in December 2021). If this opportunity is missed, the asteroid would be out of reach until late 2023, thus losing almost two years with no characterization data.

The trip time required to rendezvous with the asteroid would be too long to delay the launch of the KI until retrieving data from the rendezvous mission. The early characterization of the asteroid would

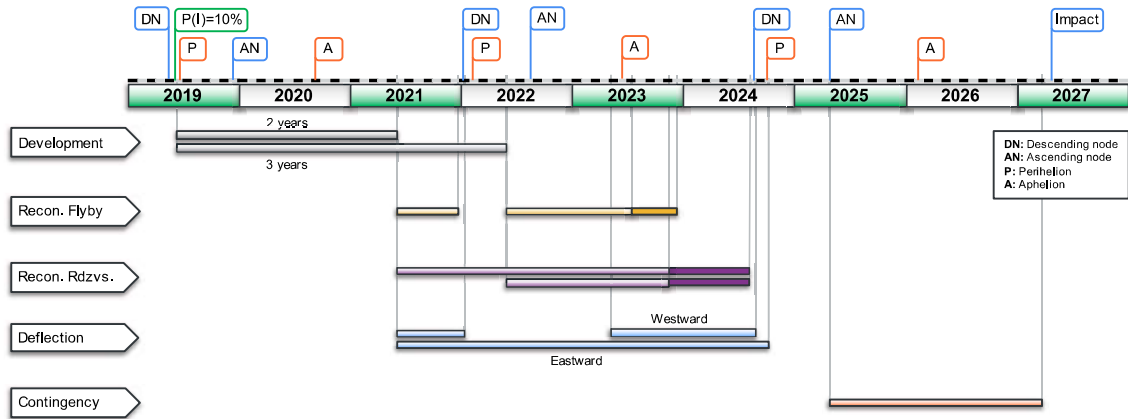


Figure 18: Timeline of the campaign

most likely rely on fast reconnaissance flybys. In any case, a spacecraft orbiting close to the asteroid can oversee the deflection process and estimate the post-deflection orbital state.

The ability to launch a KI in 2021 opens the possibility of deflecting the asteroid at its 2022 descending node, where deflections of more than one Earth radius are relatively easy to achieve. Since these missions reach the asteroid about one month after the fastest flyby missions get there, the characterization data could be processed to optimize the deflection to some extent. The high inclination of the asteroid makes westward deflection virtually impossible.

Particular attention should be paid to determining the maximum velocity change that the asteroid can sustain. This factor drives the entire design of the deflection campaign because it ultimately establishes how many KI spacecraft would be required.

The proposed campaign architecture is:

1. Launch a fast reconnaissance flyby mission in June 2021 that reaches the asteroid in December 2021 to estimate the size, shape, and possibly composition of the asteroid.
2. Launch a rendezvous mission in June 2022 (arrival in early 2024) to investigate the asteroid and monitor the deflection performance.
3. Characterize the physical properties of the asteroid to estimate its mass and the value of β . Ultimately, determine how many KI spacecraft will be required for deflection using the data retrieved by the flyby mission.
4. Launch a series of KIs in May 2023 to deflect the asteroid close to its descending node in August 2024.
5. Use the rendezvous spacecraft to determine if the deflection was successful.
6. If the deflection fails, launch a spacecraft in mid-2025 carrying a nuclear device to disrupt the asteroid one month prior to impact.

Acknowledgments

The research described in this paper was carried out at the Jet Propulsion Laboratory, California Institute of Technology, under a contract with the National Aeronautics and Space Administration.

Appendix: The geometry of the B-plane

The geometry of the asteroid-Earth encounter is better described working on the B-plane, defined as the plane normal to the incoming \mathbf{v}_∞ of the asteroid relative to Earth. Figure 19 sketches the geometry of the B-plane, where E denotes the Earth and \mathbf{v}_E is its heliocentric velocity vector. The point where the incoming asymptotic trajectory of the asteroid pierces the B-plane defines the impact point I . Öpik [14, 11] introduced a coordinate frame attached to the B-plane and centered at Earth defined by the

unit vectors $\hat{\xi}$ and $\hat{\zeta}$ (the symbol $\hat{\cdot}$ denotes unit vectors, i.e. $\hat{\mathbf{u}} = \mathbf{u}/\|\mathbf{u}\|$). The unit vector $\hat{\zeta}$ follows the direction opposite to the projection of the Earth heliocentric velocity onto the B-plane, $\mathbf{v}_{E\parallel}$:

$$\hat{\zeta} = -\hat{\mathbf{v}}_{E\parallel}. \quad (6)$$

The projected velocity of the Earth takes the form

$$\mathbf{v}_{E\parallel} = \mathbf{v}_E \cdot [(\hat{\mathbf{v}}_\infty \times \hat{\mathbf{v}}_E) \times \hat{\mathbf{v}}_\infty]. \quad (7)$$

The unit vector $\hat{\xi}$ follows from

$$\hat{\xi} = \hat{\zeta} \times \hat{\mathbf{v}}_\infty. \quad (8)$$

The location of the impact point on the B-plane is given by $\mathbf{b} = [\xi, \zeta]^T$.

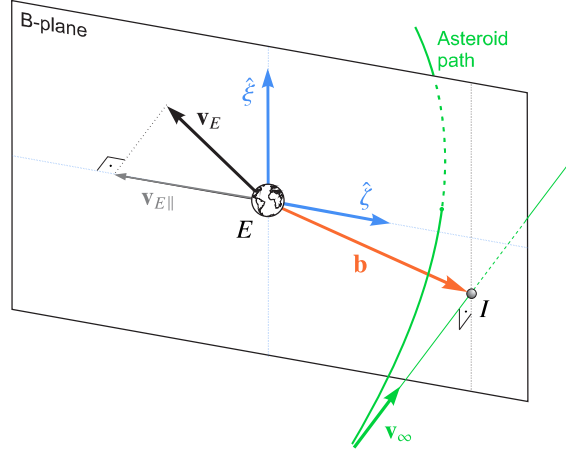


Figure 19: Geometry of the encounter and definition of the B-plane

The distance from the center of the Earth to I , $b \equiv \|\mathbf{b}\|$, is the impact parameter of the hyperbolic relative trajectory:

$$b = \frac{h}{v_\infty} = \frac{\mu}{v_\infty^2} \sqrt{e^2 - 1}, \quad (9)$$

which can be written in terms of the incoming v_∞ of the asteroid and its orbital angular momentum h or eccentricity e . The gravitational parameter of the Earth is denoted by μ .

The asteroid will impact the Earth when its perigee is lower than Earth's radius,

$$r_p \leq R_E. \quad (10)$$

The conservation of the angular momentum yields

$$h = r_p v_p = b v_\infty \quad (11)$$

and therefore Eq. (10) transforms into

$$b \leq R_E \sqrt{1 + \frac{2\mu}{R_E v_\infty^2}}. \quad (12)$$

For the case of 2019 PDC, where $v_\infty \approx 20$ km/s, the impact condition simplifies to

$$b \leq 1.15 R_E. \quad (13)$$

References

- [1] H. Melosh, I. Nemchinov, Y. I. Zetzer, Non-nuclear strategies for deflecting comets and asteroids., in: *Hazards due to Comets and Asteroids*, pp. 1111–1132.
- [2] T. J. Ahrens, A. W. Harris, Deflection and fragmentation of near-Earth asteroids, *Nature* 360 (1992) 429.
- [3] C. Bombardelli, J. Peláez, Ion beam shepherd for asteroid deflection, *Journal of Guidance, Control, and Dynamics* 34 (2011) 1270–1272.
- [4] A. Petropoulos, J. Sims, S. Bhaskaran, S. Chesley, R. Park, D. Yeomans, R. Haw, Mission design for a kinetic-energy asteroid-deflection spacecraft, in: *AIAA/AAS Astrodynamics Specialist Conference and Exhibit*, p. 6256.
- [5] M. Vasile, C. Colombo, Optimal impact strategies for asteroid deflection, *Journal of Guidance, Control, and Dynamics* 31 (2008) 858–872.
- [6] D. Grebow, D. Landau, S. Bhaskaran, P. Chodas, S. Chesley, D. Yeomans, A. Petropoulos, J. Sims, et al., Deflection missions for asteroid 2011 AG5, in: *23rd International Symposium on Space Flight Dynamics*.
- [7] A. F. Cheng, J. Atchison, B. Kantsiper, A. S. Rivkin, A. Stickle, C. Reed, A. Galvez, I. Carnelli, P. Michel, S. Ulamec, Asteroid impact and deflection assessment mission, *Acta Astronautica* 115 (2015) 262–269.
- [8] A. Cheng, P. Michel, M. Jutzi, A. Rivkin, A. Stickle, O. Barnouin, C. Ernst, J. Atchison, P. Pravec, D. Richardson, et al., Asteroid impact & deflection assessment mission: kinetic impactor, *Planetary and space science* 121 (2016) 27–35.
- [9] M. B. Syal, J. M. Owen, P. L. Miller, Deflection by kinetic impact: Sensitivity to asteroid properties, *Icarus* 269 (2016) 50–61.
- [10] S. Bhaskaran, S. Chesley, S. Park, A. Petropoulos, J. Sims, D. Yeomans, R. Haw, Navigation challenges of a kinetic energy asteroid deflection spacecraft, in: *AIAA/AAS Astrodynamics Specialist Conference and Exhibit*, p. 6254.
- [11] G. Valsecchi, A. Milani, G. Gronchi, S. Chesley, Resonant returns to close approaches: Analytical theory, *Astronomy and Astrophysics* 408 (2003) 1179–1196.
- [12] B. A. Conway, Near-optimal deflection of earth-approaching asteroids, *Journal of Guidance, Control, and Dynamics* 24 (2001) 1035–1037.
- [13] J. Roa, J. Peláez, The theory of asynchronous relative motion I: time transformations and nonlinear corrections, *Celestial Mechanics and Dynamical Astronomy* 127 (2017) 301–330.
- [14] E. J. Öpik, Collision probabilities with the planets and the distribution of interplanetary matter, in: *Proceedings of the Royal Irish Academy. Section A: Mathematical and Physical Sciences*, volume 54, JSTOR, pp. 165–199.